Vis Comput
DOI 10.1007/s00371-014-0999-1

ORIGINAL ARTICLE

3D shape creation by style transfer

Zhizhong Han · Zhenbao Liu · Junwei Han · Shuhui Bu

© Springer-Verlag Berlin Heidelberg 2014

Abstract In this paper, we propose a new style transfer method for automatic 3D shape creation based on new concepts of style and content of 3D shapes. Our unsupervised style transfer method could plausibly create novel shapes not only by recombining existent styles and contents in a set but also by combining new-coming styles or contents with the existent ones conveniently. This feature provides a better way to increase the diversity of created shapes. The process of shape creation can be summarized as two stages. First, style and content separation is performed to analyzed shapes in a set. Second, novel shapes are created by style transfer. In our setting, contents are first separated via clustering shapes using a new defined global shape distance, and then, style parts are clustered into different style classes. Specifically, style parts are extracted from each pair of intra-content shapes through comparing their multi-scale corresponding patches instead of corresponding parts. This strategy makes the process of extracting style parts become insensitive to slight geometric changes. The multi-scale corresponding patches are obtained via partitioning the two shapes in a consistent way by the proposed correspondence transfer. Meanwhile, to quantify the comparison results for locating style parts, a novel local shape difference function (LSDF) is introduced. Based on LSDF, extracting a style part from each shape is formulated as an optimal LSDF threshold selection problem. In the experiments, we test our method in several sets of man-made 3D shapes and obtain plausible created shapes based on the reasonably separated styles and contents.

Keywords Style and content separation · Style transfer · Shape creation · Local shape difference function

Z. Han · Z. Liu (✉) · J. Han · S. Bu
127, Youyi road, Xi'an, China
e-mail: liuzhenbao@nwpu.edu.cn

Z. Han
e-mail: h312h@mail.nwpu.edu.cn

J. Han
e-mail: jhan@nwpu.edu.cn

S. Bu
e-mail: bushuhui@nwpu.edu.cn

1 Introduction

Nowadays, the two terms of shapes, style and content, are used to synthesize shapes for novel shape creation [17,26,28]. In these works, novel shapes are created by recombining existent styles and contents in a set. This fashion can be seen as transferring existent styles to existent contents, which is called as existent style transfer here. Although existent style transfer is a widely accepted way of creating shapes, it limits the diversity of novel shapes by merely recombining existent styles and contents. To increase the diversity of created shapes conveniently, a new style transfer method is proposed to include another way of creating shapes which is called as new-coming style transfer. New-coming style transfer is able to use new given styles or contents without repeating the whole analysis procedure. In addition, the proposed style transfer method is based on the new concepts of style and content of 3D shapes.

The concepts of content and style defined in the previous applications differ a lot. For example, in [26], contents and styles of face pictures are represented by different poses of head and different persons, respectively; in [28], the appearance and anisotropic part scales are regarded as the content and style of 3D shapes; in [17], content and style of 2D curves are defined as the global structure and local variation, respectively. In this paper, we propose a new style of 3D shapes

Published online: 01 July 2014

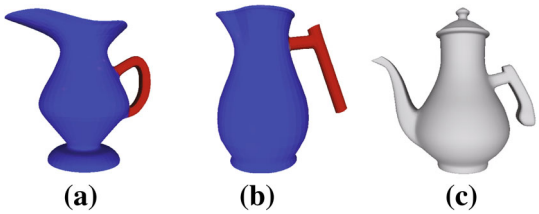

Fig. 1 The definitions of content and style. Shape **a** and shape **b** have the same content but different styles. Shape **b** and shape **c** have the same style but different contents. The *color* shown on shape **a** and shape **b** describes the dissimilarity degree between the corresponding parts. The *red* means high dissimilarity, while the *blue* means low dissimilarity. More details will be explained in Sect. 4.2.2

as the local part variation which is an extension from 2D curves in [17] to 3D shapes and define the content as the global structure in the same form as [28] and [17]. Taking the pots in Fig. 1 for example, shape (a) and shape (b) are both jugs containing approximately cylindrical bodies and without lids, while shape (c) is a flagon containing a threadlike spout and a lid. Because of the same global structure, shape (a) and shape (b) are deemed to be with the same content, by contrast, shape (c) is with another content. Meanwhile, we deem shape (b) and shape (c) belong to the same style, but shape(a) belongs to another, since shape (b) and shape (c) contain similar handles which differ from the handle of shape (a) greatly.

Before creating novel shapes, we perform style and content separation to analyze shapes in an initial set. To analyze shapes from a coarse to fine resolution, content separation is first achieved by clustering shapes using a new global shape distance. Then, style parts are clustered into different style classes.

Extracting style parts is a key work in our paper. An intuitive idea of extracting style part is to compare corresponding segmented parts of two shapes in the feature space, and then, the most dissimilar part is regarded as the style part of each shape. However, this idea has three disadvantages. The first one is that it relies on semantic segmentation which is still a challenging problem until now. The second one is that it is difficult to determine how many pairs of semantic parts to be compared. The third one is that the most dissimilar part may not be a style part since comparing shapes at part level is sensitive to slight geometric changes. For example, it is hard to distinguish desirable handle style parts of shape (a) and shape (b) in Fig. 1 since their bodies are also slightly different. The reason of this uncertainty is that the idea cannot capture the whole difference, such as the difference between the context of compared parts. Thus, to reduce dependence on semantic segmentation and the influence caused by slight geometric changes, we extract style parts from the most dissimilar regions of two intra-content shapes by comparing their multi-scale corresponding patches instead of segmented parts. The comparison process is performed between each pair of intra-content shapes since it is easier to obtain meaningful dense correspondence between similar shapes.

By comparing patches in a multi-scale way, the difference between corresponding patches as well as the difference between their context can be captured. In each shape, we accumulate the difference in all scales on each vertex to contrast the most dissimilar regions to the similar regions between two compared shapes. After shape comparison, vertices in the region containing style part will stand out with high dissimilarity degree. This is because, in most of scales, the difference between corresponding regions containing content parts is small in terms of geometric and context, while that containing style parts is big. In order to evaluate the dissimilarity degree between the corresponding regions, we quantify the difference on each vertex by a proposed local shape difference function (LSDF). Based on LSDF, style parts of compared shapes are extracted by selecting a pair of optimal LSDF thresholds. This indicates that the style part of each shape consists of vertices with higher LSDF values exceed the corresponding threshold.

The main contributions of our paper include the following:

1. We propose a novel framework of style and content separation by means of a new style of 3D shapes defined as the local part variation. Novel 3D shapes are created via transferring extracted styles to contents.
2. Style parts are extracted via comparing multi-scale corresponding patches of pairwise shapes and a new function, local shape distance function (LSDF), is introduced to quantify the difference between their local regions. The multi-scale corresponding patches are obtained by a proposed correspondence transfer which transfers the point-to-point correspondence to the patch level.
3. We develop an automatic placement method for style and content parts, which determines their stitching positions and yields relatively plausible novel 3D models.
4. In order to increase the diversity of created shapes conveniently, new-coming style transfer is introduced to use new given styles or contents without repeating the whole analysis procedure. This procedure first classifies new style parts into a similar style class and then substitutes all the existent style parts in this class by the new style part to synthesize novel 3D shapes with existent contents.

2 Overview

A set of shapes with uniform scale from a given class are taken as the input of our algorithm. The procedure of our

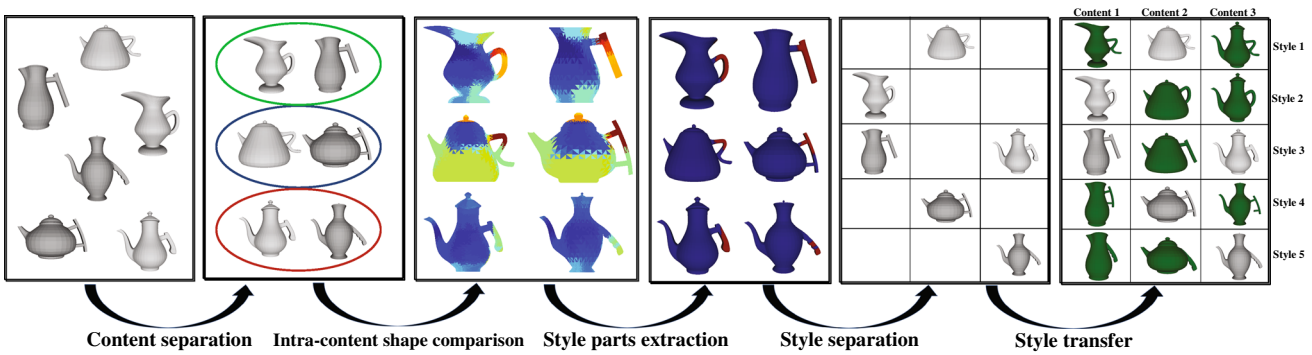

Fig. 2 An overview of our method. First, contents are separated based on a new defined global shape distance via clustering. Then, the two intra-content shapes in *green*, *blue*, and *red circles*, are compared at the patch level in a multi-scale way, respectively. In each shape, the LSDF is computed to quantify the comparison results for locating the most dissimilar regions. Then, the style part of each shape is extracted by selecting an optimal LSDF threshold. Subsequently, styles are separated by clustering style parts with D2 descriptor and shape contexts. Finally, novel shapes are created by transferring styles to the existent contents in the set

method are outlined as follows, and the overview is illustrated in Fig. 2.

1. **Content separation**: Shapes in the set are separated into different content classes via k-medoids clustering. A new global shape distance is proposed to measure the similarity between shapes.
2. **Intra-content shape comparison**: To identify the style part of each shape, we propose a new analysis method which contrasts it to another shapes in the same content class via comparing their multi-scale corresponding patches. In addition, a new function define on the mesh, LSDF is introduced to evaluate the dissimilar degree between corresponding regions.
3. **Style parts extraction**: Based on LSDF, we introduce a novel method to extract style part from each shape by a LSDF threshold. Each extracted style part is formed by vertices with higher LSDF values than the threshold. We select two optimal LSDF thresholds of compared shapes jointly, which aims to maximize the dissimilar degree between extracted style parts and minimize the similar degree between extracted content parts.
4. **Style separation**: In this step, we first refine the extracted style parts to make them as meaningful as possible. Then, D2 descriptors [18] and Shape Contexts [16] are combined to describe each refined style part. Shapes are separated into different style classes via clustering their refined style parts by k-mediods clustering.
5. **Shape creation**: Novel shapes are created via style transfer which includes two types. One type is called as existent style transfer and it creates new shapes by transferring styles to contents in the existent set. Another novel type, new-coming style transfer, creates shapes by utilizing new given styles or contents.

3 Related work

3.1 Component-based shape creation

Probabilistic graphical model, such as Bayesian network, has been used in recent works for shape creation [7,14]. This model can be trained on manually segmented shapes of a particular class with semantic labelling and context information. Novel shapes are created by sampling this model via recombining the segments. Another approach to shape creation evolves a set of shapes that are iteratively fit to a user's preferences [29]. With this scheme, novel shapes are an interpolation of the segmented input shapes. Moreover, symmetric functional arrangements are proposed to create functionally plausible model variations using the parts across different model families in [30]. These works need to segment shapes in the input set manually, and some of them have to be provided with context information or labelling. However, many manual works are time-consuming and not fully automatic. Generally, our work belongs to this category, but style parts are located and extracted by comparing the multi-scale corresponding patches automatically rather than segmenting shapes manually. Furthermore, no context information and labelling are required.

3.2 Style and content separation

There have been some works on style and content separation. Early works use different supervised learning methods to train the presumed parameterized models that represent the content and style in a set of 2D images [26,27]. Ahmed et al. [9] learn a decomposable generative model that explicitly decomposes the content from style on manifolds

representing dynamic objects. Similar ideas are implemented by statistical modeling using PCA as well [4,5]. Different from their works, we focus on separating styles and contents of 3D models.

To create 3D shapes, a recent work on style and content separation [28] defines the style as anisotropic part scales of 3D shapes and obtains the inter-style and intra-style part correspondence based on the co-segmentation method. However, novel shapes are merely created by varying scales of segments of each shape; thus, novel shapes lack diversity. In our paper, the defined style is different from [28], hence the analysis method and styles to be transferred are different in essence. Moreover, our style and content separation are achieved without recourse to semantic segmentation since many shapes with complex parts cannot always be cut into semantic segments by segmentation method [22].

To create 2D shapes with curves, Li et al. [17] perform style and content separation in a set of 2D silhouettes by analyzing a feature-shape association matrix. Although our new style of 3D shapes is a natural extension of their 2D curve's style, our framework of algorithm is completely different from theirs.

As a means of creating novel shapes by style transfer, our method not only creates new shapes via existent style transfer as performed in [28] and [17], but also continuously enlarges the set via new-coming style transfer. To increase the diversity of novel shapes conveniently, the new-coming style transfer could use new given styles or contents without repeating the whole analysis procedure. This is achieved by fully exploiting the initial results of style and content separation. Moreover, it demonstrates the extendible feature of our style transfer which is similar as the "Translation" functionality mentioned in the pioneering work [26].

3.3 Shape comparison

A similar work to our style part extraction is selecting distinctive regions of a 3D shape in [24], but the objective is different from ours. The distinctive regions of one shape are selected to distinguish the shape from objects of a different type, while we aim to locate and extract style parts of two intra-content shapes. Another similar work develops a novel formulation for the notion of shape differences by a difference operator in [21]. The difference operator needs to be derived from a functional map based on the eigenvectors of the Laplacian matrix proposed in [20]. However, we locate the difference between shapes by comparing their corresponding patches in a multi-scale way. This strategy could resist on the influence caused by slight geometry changes, and moreover, it has the ability to compare two rigid shapes that are not isometric.

4 Style-content separation

Shapes to be analyzed consist of man-made triangle meshes with various contents and styles. The objective of this section is to separate contents and styles of shapes in a set under the challenges of different shape structures and various local part variations. We also introduce a novel LSDF to help recognize style parts.

4.1 Content separation

In this step, we expect to separate shapes into content clusters according to their global structures. Since all shapes are from the same object class and the potential intra-content shapes may contain geometric changes, it is hard to separate shapes into content clusters by the traditional global feature distance. Our solution is to define a new global shape distance which combines Hausdorff distance [6] with the traditional global feature distance.

The Hausdorff distance evaluates the similarity between shapes in term of local features. We choose Wave Kernel Signature (WKS) [2] as the local feature. The WKS arises from studying the Schrödinger's equations governing the dissipation of quantum mechanical particles on the geometric surface. Considering a quantum particle with unknown position and different energies on the surface, the WKS of each vertex describes the average probability of measuring the quantum mechanical particle at this specific vertex on the surface. By varying the energy of the particle, the WKS encodes and separates information from various different Laplace eigenfrequencies. Thus, in this paper, the Hausdorff distance is used to measure the difference between shapes in term of dissipation features.

By capturing the difference between dissipation features, the Hausdorff distance enlarges the distance between inter-content shapes. Moreover, the WKS is a Laplacian-based feature, and it is robust to small non-isometric deformations [2]. This fact shortens the Hausdorff distance between intra-content shapes by reducing the influence caused by their slight geometric changes. Therefore, the Hausdorff distance makes up for the deficiency of traditional global feature distance, which makes the new global shape distance become more discriminative to separate contents.

The traditional global feature distance measures the difference between shapes in term of Eigen value descriptor (EVD) [13]. Each shape is represented globally by the eigenvalues of the geodesic affinity matrix. In our setting, the second to the tenth largest eigenvalues are used to form a feature vector denoted as $evd()$. The proposed distance measure $d(X, Y)$ between two arbitrary shapes X and Y is the combination of the traditional global feature distance $d_{evd}(X, Y)$ and the Hausdorff distance $d_{wks}(X, Y)$ as Eq. 1. Content separation is achieved by k-medoids clustering using $d(X, Y)$ as

the distance measure.

$$d(X, Y) = \lambda * d_{evd}(X, Y) + d_{wks}(X, Y) \quad (1)$$

$d_{evd}(X, Y)$ is defined as the L2 norm of vector subtraction between $evd(X)$ and $evd(Y)$ as defined in Eq. 2. $d_{wks}(X, Y)$ is defined as Eq. 3, where $d(x, y) = \|wks(x) - wks(y)\|_2^2$, and $wks()$ is the WKS of each vertex. The parameter λ is set to 0.01 in all experiments.

$$d_{evd}(X, Y) = \|evd(X) - evd(Y)\|_2 \quad (2)$$

$$d_{wks}(X, Y) = \max\left\{\max_{x\in X}\left\{\min_{y\in Y} d(x, y)\right\}, \max_{y\in Y}\left\{\min_{x\in X} d(x, y)\right\}\right\} \quad (3)$$

The number of content clusters is determined by clustering validation [10]. The purpose of clustering validation is to select an optimal number of clusters from several candidate numbers in term of metrics. Specifically, we obtain a content clustering result with each candidate number, and then the metrics is used to evaluate how well the contents are separated into the specified candidate number. The candidate number with the biggest metrics value will be selected as the optimal number of content clusters. The involved metrics is Dunn index [10] which assigns big score to the clustering result that produces clusters with high intra-cluster similarity and low inter-cluster similarity.

4.2 Intra-content shape comparison

To extract style parts, two intra-content shapes are compared at the patch level in a multi-scale way. The dissimilar degree is quantified by a scalar value function, LSDF, which sums up the dissimilarity between multi-scale corresponding patches on each vertex. Two compared shapes form a comparison pair, one of them is regarded as a target shape (shape T) and the other is regarded as a reference shape (shape R).

To locate and extract style parts, the comparison should have two properties. First, the comparison between corresponding patches is performed in several scales, and the number of patch pairs is increased gradually in each scale. This property means the size of patches is changing from big to small for capturing the difference between corresponding regions in term of geometric and context. Second, in each scale, the corresponding patches should have a similar size and locate at the similar relative position on each shape. This property guarantees that we are comparing the corresponding regions of two shapes with similar size.

According to these properties, two steps are required to prepare for the comparison. The first step is to partition the two shapes into patches in a consistent manner. This step aims to reduce the difference caused by the size and the location of potential corresponding patches. The second step is to establish the correspondence between these patches. In the following subsection, we describe our solution of obtaining this kind of multi-scale corresponding patches which require to partition two compared shapes in a consistent manner as a prior.

4.2.1 Obtaining multi-scale corresponding patches

A traditional flow of obtaining corresponding patches includes the following steps. First, partition each shape into patches separately, and then, find the correspondence in the feature space. However, this flow is not suitable for comparing corresponding regions to extract style parts, because it cannot partition the two different shapes in a consistent manner. For example, the two shapes in Fig. 3a are partitioned into 20 patches, respectively; however, it is hard to quantify the dissimilarity between corresponding regions by comparing patches.

In each scale, to partition two shapes in a consistent way, we propose to partition shape R into patches as a template first and then partition shape T in the same way as the template. Specifically, shape R is partitioned by spectral clustering; then a proposed method, correspondence transfer, is used to partition shape T. In addition, correspondence transfer establishes the patch-to-patch correspondence along with partitioning shape T. The point-to-point correspondence between vertices of the two shapes is transferred to the multi-scale patch level by correspondence transfer. The corresponding patches obtained in a specified scale by correspondence transfer are shown in Fig. 3b, and they meet the requirements of comparing corresponding regions. The details of the aforementioned process are listed below:

1. **Point-to-point correspondence**: For each comparison pair, point-to-point correspondence is first established between the two sets of vertices. It provides the source correspondence for correspondence transfer in all scales. The point-to-point correspondence is established through an injective mapping function Φ symbolized as $\Phi : T \rightarrow R$. As EVD is used to describe shapes to separate

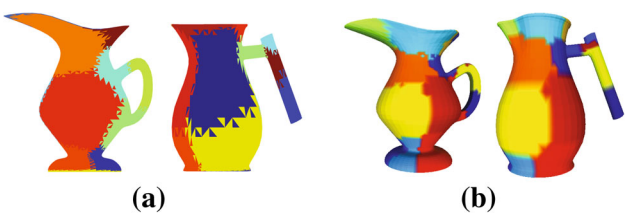

Fig. 3 **a** The patches obtained via partitioning shapes by spectral clustering, respectively; the *color* of each patch does not indicate patch correspondence. **b** Corresponding patches obtained by correspondence transfer. The *color* of each patch shows correspondence information

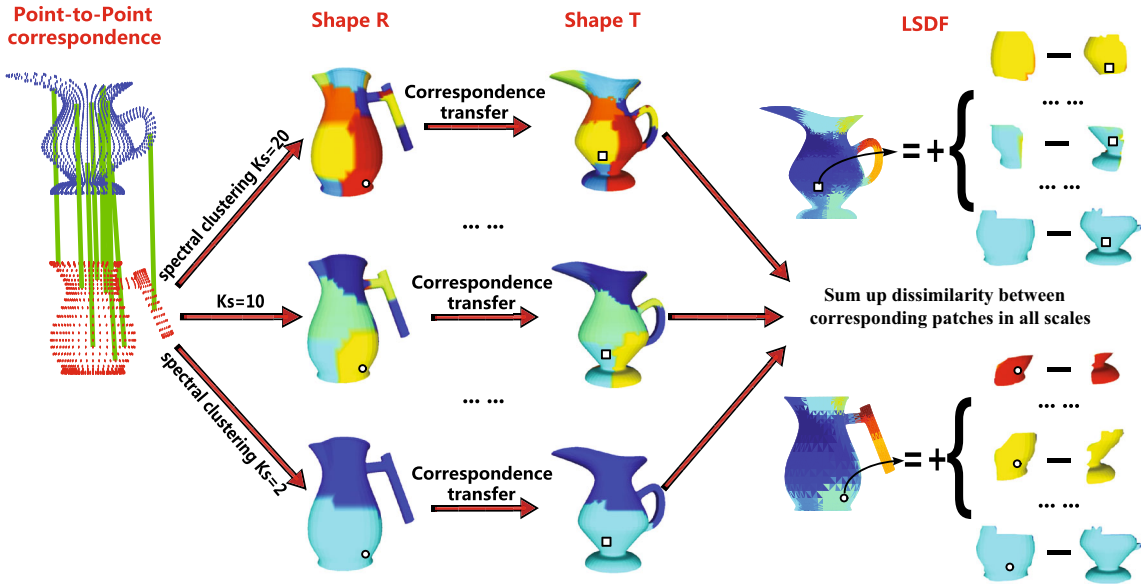

Fig. 4 The process of comparison at the patch level, where the point-to-point correspondence is shown briefly

contents, here, for saving computation cost, we also resort to the spectral method [12] to obtain Φ in the spectral domain.

The method in [12] operates on spectral embeddings obtained from eigenvectors of geodesic affinity matrix so as to normalize them with respect to uniform scaling and rigid-body transformation. Then, non-rigid alignment and proximity-aided matching are used between the two sets of spectral embeddings. Specifically, non-rigid alignment is performed for optimizing a global correspondence cost. However, it is hard to distinguish between near-by points in the dense correspondence. To improve correspondence locally, proximity-aided matching is used with selecting some anchor points pairs. Anchor points pairs are points that are best matched. Based on the anchor pairs, the correspondence cost of arbitrary two points is defined via combining L2 distance between their spectral embeddings with the difference between their geodesic proximities to these anchor points. In our experiments, we select four pairs of anchor points to establish a meaningful Φ. In Fig. 4, Φ is briefly demonstrated in the leftmost column. The shape with blue vertices is T, and the one with red vertices is R.

2. **Partition shape R**: In each scale s, faces of R are merged into K_s patches via spectral clustering. The partitioned R provides a template for partitioning T. An affinity matrix is first constructed by the connectivity of vertices on R. The entry of the affinity matrix is either one or zero, which indicates whether two vertices are connected by an edge. In the second column from the left of Fig. 4, shape R is partitioned into patches via spectral clustering in multi-scale; the results are shown in scale $K_s = 20$, $K_s = 10$ and $K_s = 2$. Each patch on R is labeled as P_m^s, where $m \in \{1, 2, \cdots, K_s\}$.
3. **Correspondence transfer**: In each scale s, partitioning T and establishing patch-to-patch correspondence between T and R are implemented by correspondence transfer. Constrained by point-to-point correspondence Φ, shape T is first partitioned into K_s' patches in a consistent way as partitioning shape R. Then, the patch-to-patch correspondence Ψ_s is established accordingly. As Φ, Ψ_s is also an injective mapping, such that $\Psi_s : T \rightarrow R$.

Specifically, to partition shape T, correspondence transfer uses an inference, that is, if a set of vertices on R are the same patch, then their corresponding vertices on T are going to form a patch too. For example, assuming a set of vertices R_j belongs to patch P_m^s on R, then the inference forms a patch Q_n^s on T by the corresponding vertices of R_j, $\Phi^{-1}(R_j)$, where $\Phi^{-1}(R_j) \in Q_n^s$. In this way, T is partitioned into patches Q_n^s as partitioning shape R, where $n \in \{1, 2, \ldots, K_s'\}$.

Moreover, correspondence information from Φ is transferred to the patch level by establishing Ψ_s, such that $\Psi_s(Q_n^s) = P_m^s$. In the third column from the left of Fig. 4, correspondence transfer partitions shape T in a consistent way as partitioning R along with establishing Ψ_s.

4.2.2 Quantify shape comparison

After obtaining the corresponding patches in each scale, we perform shape comparison by comparing each pair of corresponding patches via computing their distance in the feature space. The result of shape comparison is quantified by summing up the dissimilarity between corresponding patches

in all scales. A vertex-based scalar function, LSDF, is used to quantify the dissimilarity degree between corresponding regions of two shapes.

Assuming that shape (a) and shape (b) in Fig. 1 form a comparison pair, the desirable comparison result evaluated by LSDF is illustrated with color. The red part of each shape consists of vertices with high LSDF values, which represents high dissimilarity degree between the two red parts; while the blue part consists of vertices with low LSDF values, which represents low dissimilarity degree between the two blue parts.

The feature of each patch is the combination of the normalized sum of WKS and Shape Contexts (SC). The WKS of each vertex has been explained in Sect. 4.1, and here SC of each vertex is calculated to capture its spatial context. The feature of a patch X is denoted as Eq. 4, where num is the vertex number in patch X. $D(X)$ is formed by a 100-dimensional WKS vector and a 3375-dimensional SC vector.

$$\mathbf{D}(X) = \left\{ \frac{1}{num}\sum_{i\in X} wks(i) \quad \frac{1}{num}\sum_{i\in X} sc(i) \right\} \tag{4}$$

The computation processes of LSDF on shape T and shape R are slightly different since the patch-to-patch correspondence Ψ_s is an injective mapping from T to R. In each scale s, LSDF of each vertex on T and R is defined as Eqs. 5 and 6, respectively.

$$\mathrm{LSDF}^s(T_i) = \|\mathbf{D}(Q_n^s) - \mathbf{D}(\Psi_s(Q_n^s))\|_2^2 \tag{5}$$

where $T_i \in Q_n^s$. $\mathrm{LSDF}^s(T_i)$ is the difference between the patch Q_n^s and its corresponding patch $\Psi_s(Q_n^s)$.

$$\mathrm{LSDF}^s(R_j) = \begin{cases} \|\mathbf{D}(P_m^s) - \mathbf{D}(\Psi_s^{-1}(P_m^s))\|_2^2 & \text{if } \Psi_s^{-1}(P_m^s) \text{ exist}, \\ \min\limits_{n\in[1,K_s']} \mathbf{D}(P_m^s) - \mathbf{D}(Q_n^s)\|_2^2 & \text{otherwise}, \end{cases} \tag{6}$$

where $R_j \in P_m^s$. $\Psi_s^{-1}(P_m^s)$ denotes the corresponding patch of P_m^s. For the patch on R that no patch on T corresponds to, the LSDF^s values of vertices in it are the distance between it and its most similar patch on T.

LSDF of each vertex on T or R is the sum of LSDF^s in all scales as Eq. 7. In Fig. 4, the computation process of LSDF is shown in the rightmost column. The black circle and black square represent a vertex on R and a vertex on T, respectively. Take the black square for example; its LSDF value is equal to the sum of dissimilarity between two corresponding patches in all scales. In each scale, one of the two corresponding patches is the patch that the square belongs to. The LSDF of the two shapes are similar as the idealized comparison result of shape (a) and shape (b) in Fig. 1.

$$\mathrm{LSDF}(T_i \ or \ R_j) = \sum_{s=1}^{S} \mathrm{LSDF}^s(T_i \text{ or } R_j) \tag{7}$$

4.3 Style part extraction

The objective of computing LSDF is to locate the region containing style part of each shape. In this section, we consider extracting style part from the region with high LSDF values. Here, extracting style part is solved by an optimization which selects a pair of LSDF threshold jointly via considering the following three aspects.

First, it is expected to contrast each pair of shapes to filter out their own style parts. The larger their difference is, the easier style parts are extracted. On the contrary, it is desirable for their content parts to be as similar as possible. Second, the two style parts should be extracted accurately, and this is reflected from the area proportions of style part and content part. The second aspect will confine selecting big but not accurate style part to meet the first aspect. Third, LSDF values of vertices in style part should have relatively high contrast with the ones of vertices in content part. Based on the above aspects, the objective function is constructed as follows:

$$\begin{aligned} \arg\min_{\substack{C_t, S_t \in T \\ C_r, S_r \in R}} & \frac{m(C_t) * m(C_r) * \|\mathbf{D2}(C_t) - \mathbf{D2}(C_r)\|_2^2}{a(C_t) * a(C_r)} \\ & - \frac{m(S_t) * m(S_r) * \|\mathbf{D2}(S_t) - \mathbf{D2}(S_r)\|_2^2}{a(S_t) * a(S_r)}, \end{aligned} \tag{8}$$

where C_t and C_r are the potential content parts of T and R, S_t and S_r are the potential style parts of T and R. $m(X)$ is the mean of 10 minimum LSDF values in part X, and $a(X)$ represents the surface area proportion of part X. $\mathbf{D2}(X)$ is the D2 distribution [18] of part X. Essentially, D2 distribution is the histogram of pairwise Euclidean distances between the points uniformly sampled from the surface. It measures global geometric properties of an object. The dimensional of D2 vector is 40.

In order to solve the above optimization problem, an adaptive way is deployed to select two optimal thresholds, which minimizes the objective function by splitting each shape into two parts. For each comparison pair, the optimal thresholds of T and R are selected among three pairs of candidate thresholds jointly. The candidate thresholds are obtained via three famous methods. The first method is grey-level histogram from Otsu [19]; the second method computes thresholds using equation as $\sqrt{2 * ln(X)}$, where X is the vertex number of T or R; the third method is the minimax thresholding [8]. The two shapes are cut into style parts and content parts by each pair of candidate thresholds respectively. On each shape, vertices with higher LSDF values than the corresponding threshold comprise the style part(S_t or S_r); meanwhile,

the remaining vertices comprise the content part(C_t or C_r). Finally, the two style parts are extracted by selecting one of the three pairs of thresholds which minimize Eq. 8.

4.4 Refined style part

The extracted style parts may be not as semantic as they supposed to be and their boundaries may be irregular, such as the red part in Fig. 5a. To obtain reliable part features for style separation and reasonable boundary for style transfer, we refine the extracted style parts. In each shape, the boundary between extracted style part and extracted content part is adjusted by Gaussian Mixture Models (GMM) and Graphcut [15].

Our strategy is to re-classify vertices in the region near the boundary so that the style part is refined further to be more reasonable. Specifically, the vertices to be re-classified locate within 20 % of the longest geodesic distance from the extracted boundary, and they are located in the green region in Fig. 5b. Each selected vertex i is described by a two-dimensional vector including its LSDF value and SDF value [23] which is denoted as [LSDF(i) SDF(i)]. Then, GMM with two Gaussian components are fit using these feature vectors via the Expectation–Maximization (EM) algorithm. The GMM assign each selected vertex to style part and content part x_i in the form of probability $P(i|x_i)$. In Fig. 5c, the probability of assigning vertices to style part is shown in color. The vertices in red region indicate that they belong to style part with high probability. Finally, the selected vertices are re-classified into refined style part and refined content part along with adjusting the boundary by Graphcut as shown in Fig. 5d. The Graphcut minimizes the following energy functional Eq. 9, which is built from the data term e_1, and the smoothness term e_2:

$$E = \sum_{i \in \text{Selected}} e_1(i, x_i) + \omega * \sum_{(i,j) \in \text{Connected}} e_2(x_i, x_j) \quad (9)$$

$$e_1(i, x_i) = -\log(P(i|x_i) + \varepsilon) \quad (10)$$

$$e_2(x_i, x_j) = \begin{cases} -\log(|\text{SDF}(i) - \text{SDF}(j)| + \varepsilon) & x_i \neq x_j \\ 0 & x_i = x_j \end{cases} \quad (11)$$

In Eq. 9, ω is a parameter defining the degree of smoothness. Equation 10 is used to put the new boundary in the region containing big SDF changes. The result of the Graphcut algorithm is a smooth partitioning of the selected region, clearly isolating a more meaningful style part than the extracted one as shown in red parts in Fig. 5a, d. The refining process provides parts with reasonable boundary for style transfer. In the following, to avoid confusion, we still use style part and content part to refer to the refined style part and the refined content part.

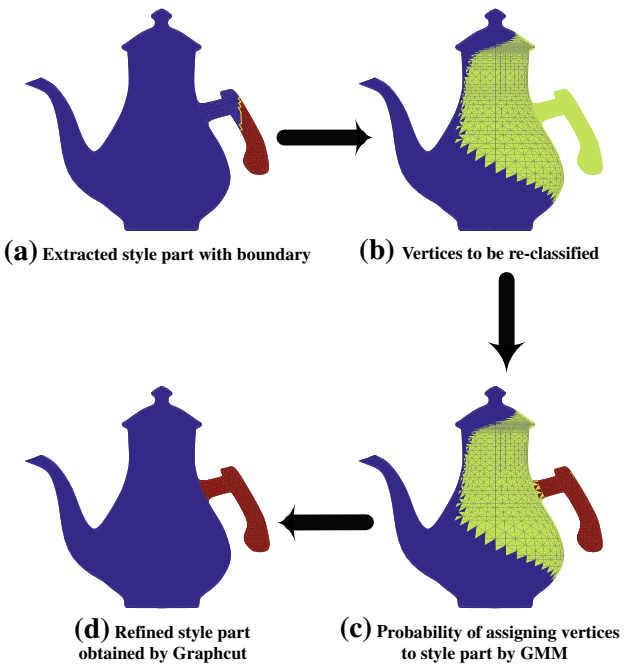

Fig. 5 The process of refining extracted style part

4.5 Inter-content style parts correspondence

To guarantee the following style separation to be significative, we should make sure all the inter-content style parts have correspondence. We select one shape from each content class randomly, and align one of selected shapes to the others by ICP method [3], respectively. Specifically, each aligned shape is represented by the geometric centers of content part and style part. If the geometric centers of style parts in each aligned pair are the nearest neighbors in term of coordinates, the two style parts are deemed to have correspondence. In this way, inter-content style correspondence is obtained through the set.

4.6 Style separation

When separating styles, D2 distribution and the normalized sum of shape contexts are combined to describe each style part. The similarity between style parts are measured by Euclidean distance. The length of D2 vector is 40, and the length of shape contexts is 3375. Style separation is achieved by k-medoids clustering, and the number of style clusters is determined by clustering validation as determining the number of content clusters.

5 Style transfer

Style transfer resolves how to use the results of style and content separation to create novel shapes automatically. In this paper, shape creation is realized at the part level via combining a content part and a style part by style transfer. The involved two parts are selected from a specified content class and a specified style class, respectively. In order to make a created shape plausibly, we have to deal with two challenges when performing style transfer. First, how to place a content part and a style part from different source shapes? Second how to stitch the two parts? Next, we will describe our solutions to the two challenges.

5.1 Placements of style part and content part of a created shape

We adopt rigid ICP [3] to determine the placement of style part and content part of a created shape according to three cases. In each case, the process of alignment is performed via two steps. The first step performs coarse alignment which aligns two parts or two source shapes coarsely. The second step performs fine alignment which adjusts the location of style part and content part of the novel shape by aligning their boundaries. Here, the boundary also denotes the border adjoining the content part and the style part of each source shape. The boundary alignment is performed through aligning two sets of points. Each set of points contains not only the points on the boundary but also the geometric center of the source shape. The geometric center is regarded as a constraint to prevent the boundary from turning over in the process of fine alignment.

The first case is shown in Fig. 6a, where a novel shape D is created with the help of other three shapes A, B and C. To increase alignment accuracy, we place the content part and style part of D in an indirect way. We use shape B as a bridge connecting shape A and shape C. Shape B has the same content as shape A and the same style as shape C. Then, we align the style part (in red) of C to the style part (in red) of B so as to obtain a transformation matrix M_1. The coarse placement of content part (in green) of D is determined by performing rigid transformation on the content part (in green) of C according to the transformation matrix M_1. Similarly, we align the content part (in red) of A to the content part (in red) of B so as to obtain another transformation matrix M_2. The coarse placement of style part (in blue) of D is determined by performing rigid transformation on the style part (in blue) of A according to the transformation matrix M_2.

However, if B is unknown, the second case is introduced to place style and content part of the novel shape which is created by exchanging the content part and style part of A and C. Fig. 6b shows the second case. In this case, shape C is aligned to shape A globally in the coarse alignment step, which is different from individual style part alignment and content part alignment used in the first case.

The third case is designed for creating novel shapes using a new style part or a new content part without repeating the whole analysis procedure. With fully exploiting the initial result of style and content separation, the new shape part is combined with all complementary shape parts in the existent set to form novel shapes. If the new-coming shape includes new style and new content at the same time, the third case is equivalent to the second case. If the new-coming shape includes only one new factor, taking the new style for example as shown in Fig. 6c, the style part of shape C is first classified into the most similar style class by K nearest neighbor classifier ($K = 3$). This is achieved via comparing the new-coming style part with all style parts in the set in term of the D2 descriptor and the normalized sum of shape contexts.

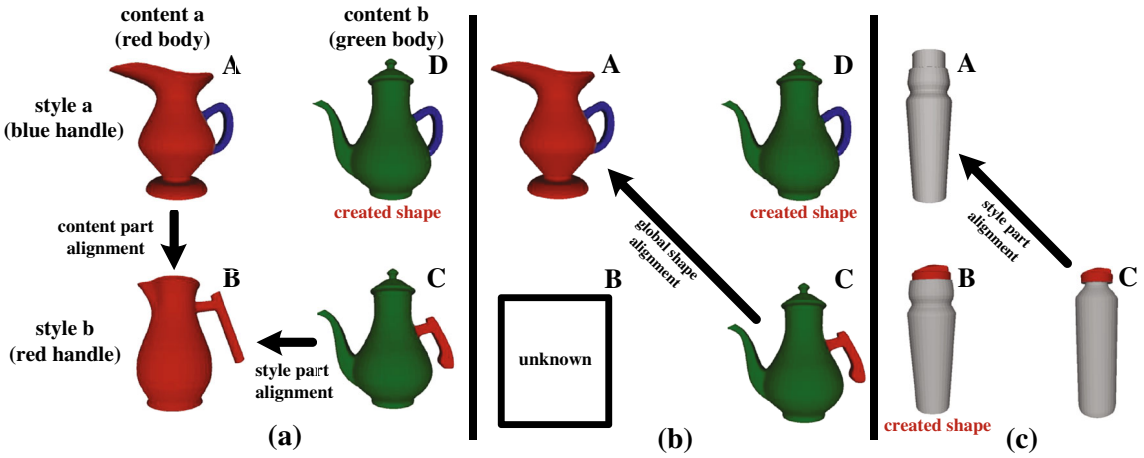

Fig. 6 The placements of style part and content part of the created shape are determined via aligning by rigid ICP. **a** The first case. **b** The second case. **c** The third case

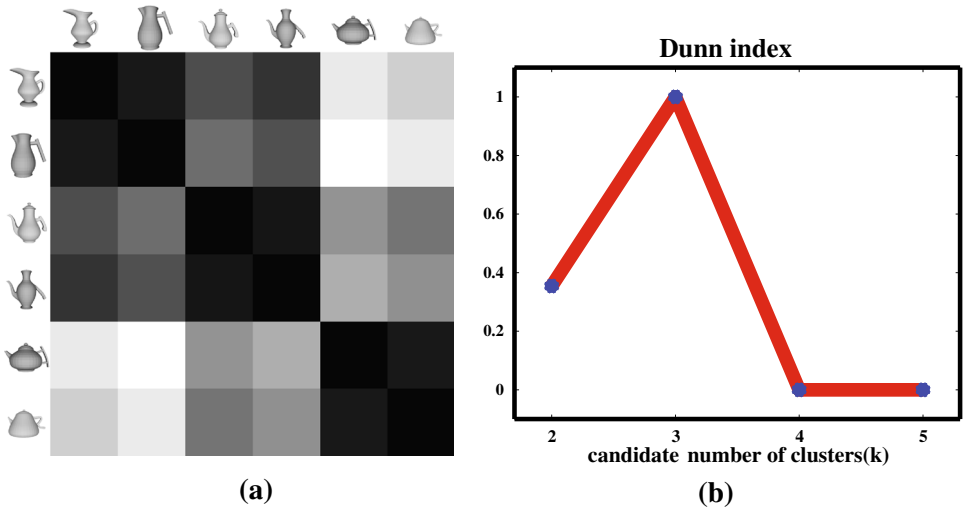

Fig. 7 **a** The affinity matrix of shapes in the teapot set. The darker the cell in the matrix, the closer the two shapes. **b** Dunn index is used to determine how many content clusters actually exist

Then, the new-coming style part replaces all the style parts in the same style class via coarse alignment. In Fig. 6c, the style part of shape A is replaced by the new style part of shape C; then, a novel shape B is created. A similar process is performed when the new-coming shape includes only a new content.

The three cases are suitable for different situations of creating novel shapes. The first two cases are designed for existent style transfer, while the third case is specially designed for new-coming style transfer with one new given style or content.

Actually, the second case could handle all the placements of parts of novel shapes obtained by existent style transfer, while the reason of designing the additional first case is that we want to place the parts of novel shapes as plausibly as possible. This requires each alignment has to be performed between similar parts to the greatest extent. Thus, novel shapes are created according to the first case with high priority, since the part alignments are all performed in the same content cluster or in the same style cluster.

5.2 Part stitching

Part stitching is not our focus; thus we merely merge a style part and a content part into a complete shape via connecting their paired boundaries. The automatic stitching process includes the following steps: first, the correspondence between the two sets of vertices on the boundaries are established by matching their relative position on each ring. Second, corresponding vertices are connected by edges, respectively. For the boundary that does not have a partner to become a pair, we will fill it as a hole. Readers can refer to recent advanced part stitching methods [11] and [1] to obtain further reasonable effects.

6 Results

In this section, we show experimental results of style and content separation and shape creation by style transfer in several sets of shapes. In the experiments, the sets of man-made shapes include goblets, teapots and sport bottles.

Content separation. We show the experimental results of content separation in the set of teapots. Their affinity matrix describes separation effect, as shown in Fig. 7a. Darker color indicates the two shapes have more similar content. Shapes are clustered into different content categories with their affinity matrix, and the cluster number is set automatically according to Dunn index. The optimal cluster number is the candidate number with the largest Dunn index. Figure 7b represents the relationship between metrics values and candidate cluster numbers. The optimal number of content cluster is consistent with the ground truth.

Correspondence transfer. We present several results of correspondence transfer, as shown in Fig. 8a. In this scale, K_s is equal to 20 in all comparison pairs. The resulting corresponding patches in each comparison pair are marked in the same color. It can be seen that correspondence transfer partitions each pair of shape T and shape R in a consistent way and establishes meaningful patch-to-patch correspondence although shapes contain different style parts. In addition, the obtained patch-to-patch correspondence is suitable for comparing regions with similar relative positions on shapes.

Style part extraction. We present the results of style part extraction for the three sets. Before extracting style parts in these sets, a range of patch numbers is set for each set in order to be adaptable for different sizes of style parts. For example, we set 2,4,…,20 and 6,8,…,20 and 8,10,…,20 as the patch number variation ranges which represent scales for the

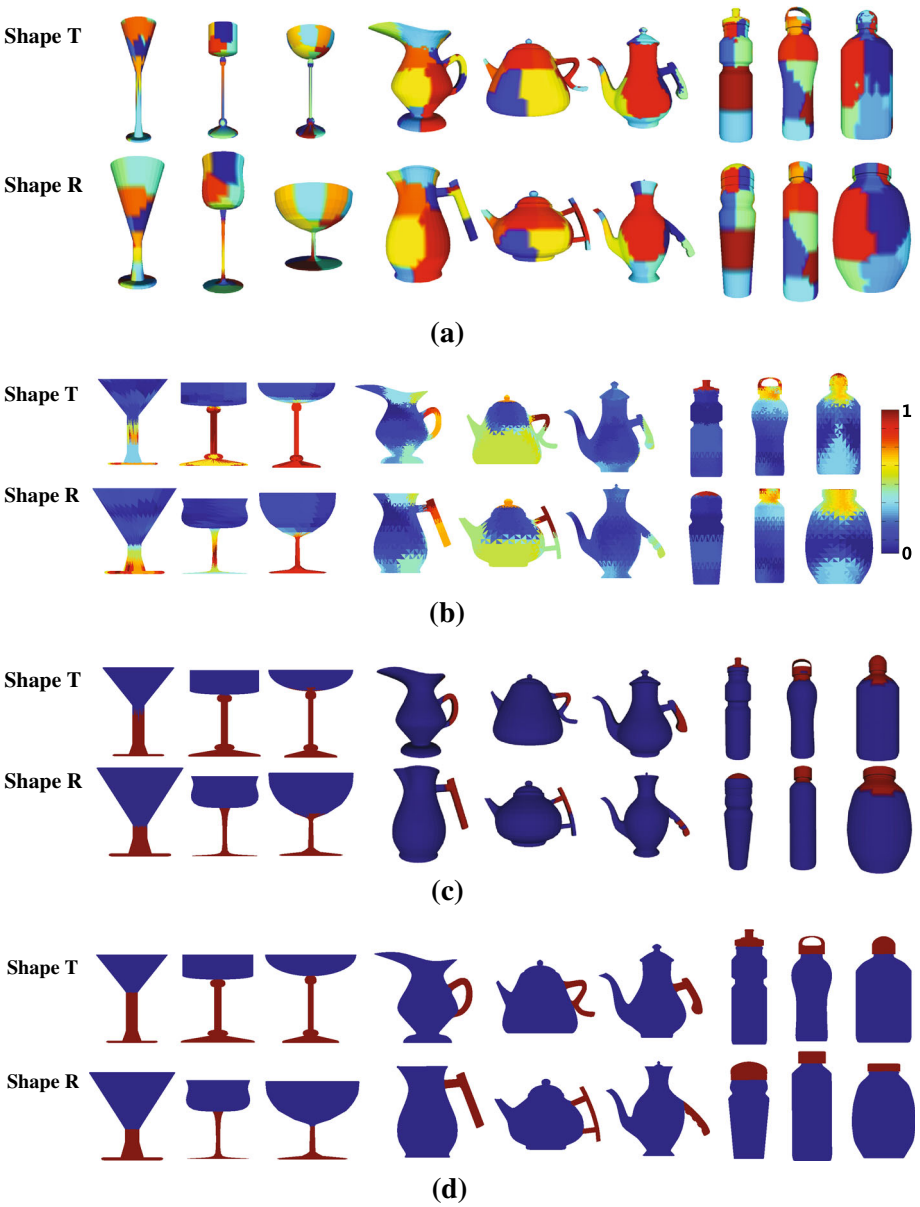

Fig. 8 The two shapes in each column consist of a comparison pair. **a** The patch-to-patch correspondence in the scale $K_s = 20$. **b** The LSDF of each shape after comparison. **c** The extracted style part and content part of each shape are marked in *red* and *blue*, respectively. **d** The refined style part and content part of each shape are marked in *red* and *blue*, respectively

sets of goblets, teapots and sport bottles, respectively. After performing pairwise shape comparisons, the LSDF of each shape in these sets is shown in Fig. 8b. The region with high LSDF values of each shape contains style part. According to solution of the optimal problem mentioned in Sect. 4.3, the style part of each shape is extracted, as shown in Fig. 8c. These results validate the first two contributions in Sect. 1. The refined style parts and content parts are shown in Fig. 8d.

Style separation. We present style separation results of the goblet set. Refined style parts are clustered according to their feature distances which are indicated by an affinity matrix, as illustrated in Fig. 9a. Dunn Index is adopted to evaluate the results of clustering styles into candidate numbers in Fig. 9b. The optimal number of style clusters is obtained with the highest Dunn index value. In this example, the style cluster number is set to three automatically.

3D shape creation by style transfer. The results of 3D shape creation by style transfer are exhibited for the three sets, respectively. In Fig. 10, we see that the goblets are reasonably separated into clusters in term of different styles and contents. Goblets in green out of the red frame are novel shapes created by existent style transfer. When new goblets (in blue frames) with new given content part or style part are provided sequentially, the goblets in green appeared in the red frame are created by new-coming style transfer. We also test our algorithm in the teapots set and sport bottles set, and

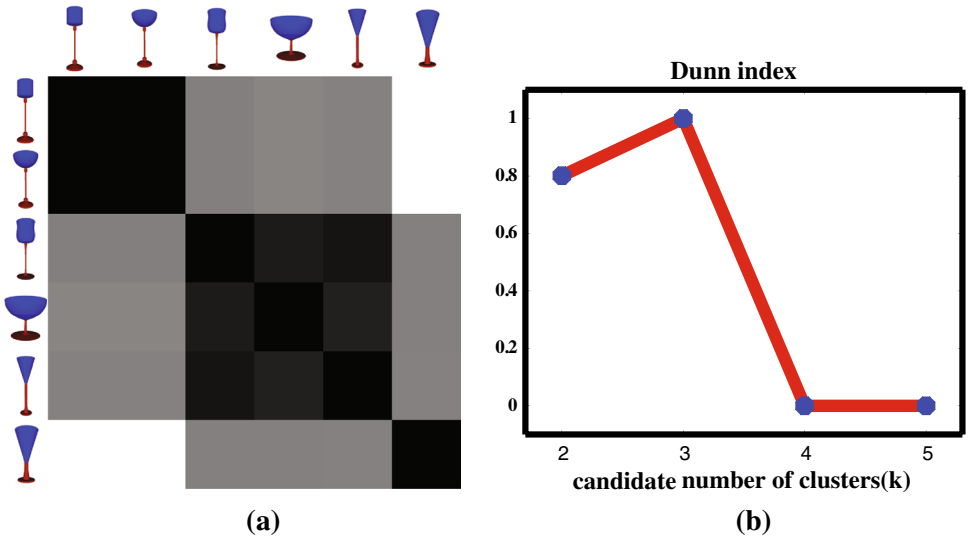

Fig. 9 **a** The affinity matrix of the refined style part marked in red in each shape. **b** Dunn index is used to determine how many style clusters actually exist

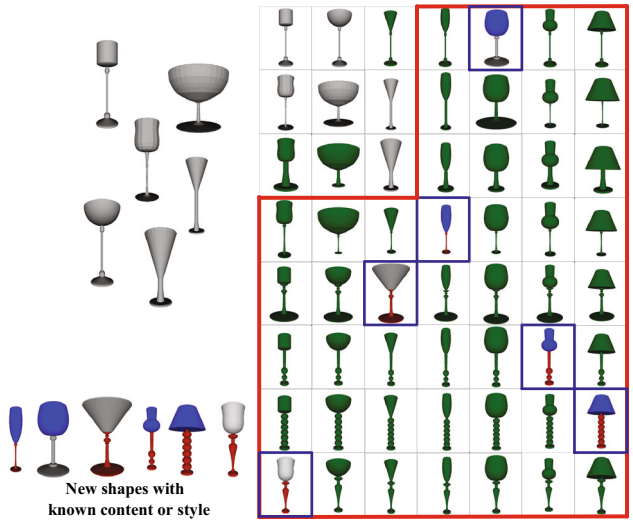

Fig. 10 The results of style and content separation and novel shape creation for goblet set (*row* style, *column* content). The novel shapes are marked in *green*. The novel shapes in the *red frame* are created by new-coming style transfer; the others are created by existent style transfer

we all get satisfactory results as shown in Fig. 11. The results shown in Figs. 10 and 11 demonstrate the capability of our algorithm in separating style and content and generating reasonable shapes by style transfer. These results validate the last two contributions in the Sect. 1.

Comparison with previous applications. Due to the different definitions of style and content, it is hard to compare our method with other similar applications quantitatively, such as [28] and [17]. However, new-coming style transfer is our advantage over previous applications. It provides a new way to enhance the diversity of created shapes via using new styles and contents conveniently.

7 Discussions, limitations and future work

Discussions. In this paper, we consider local part variation as a style of 3D model and discuss the feasibility of creating novel shapes based on separating styles and contents in a set. This is a preliminary attempt to separate styles from a set of shapes by analyzing the set without utilizing semantic segmentations of shapes. The unsupervised process depends on comparing each pair of intra-content shapes at the patch level in a multi-scale way and fully exploits their difference. Capturing the difference is converted to solve the problem of style part extraction. 3D novel shapes are created by means of automatically transferring style to other contents in the set. We are able to enlarge the set continuously and enhance the diversity of novel shapes using new-coming styles or contents without repeating the whole analysis procedure. It is worth mentioning that there are few parameters needed to be set throughout our method.

Limitations. An obvious limitation is that our method cannot analyze non-rigid shapes and shapes with significant variations. On the one hand, this limitation lies in the discriminative ability of our new defined global shape distance measure in the content separation. Since our distance measure cannot learn from training examples, recognition of the same content among similar shapes has to depend on geometric distance without any semantics. For example, global feature distance and local feature distance can be employed. On the other hand, our shape comparison strategy is based on the dense correspondence; however, it is difficult for the state-of-the art dense correspondence to establish correspondence between shapes with large geometric variations. Thus, it is a big challenge for our method to handle shapes in the Princeton Shape Benchmark [25] which contains non-rigid shapes and complex shapes. In addition, our method

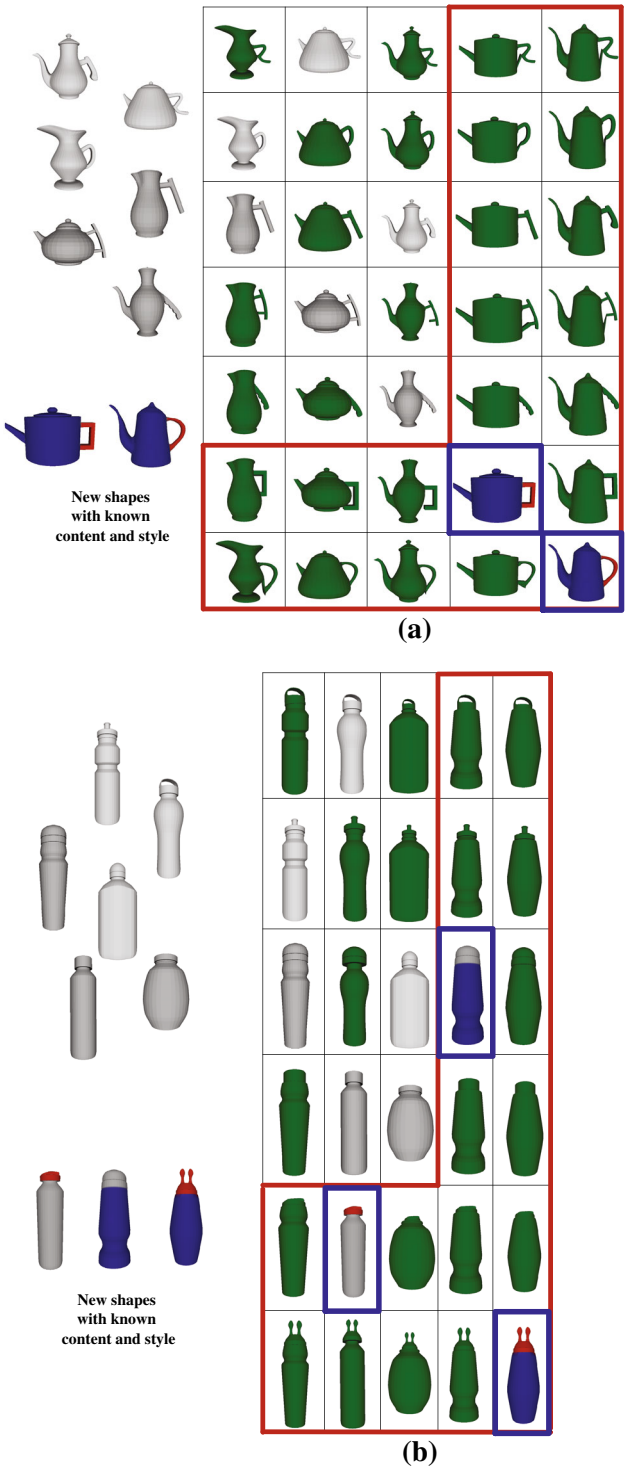

Fig. 11 Style and content separation and novel shape creation for teapot set in **a**, and sport bottle set in **b** (*row* style, *column* content). The novel shapes are marked in *green*. The novel shapes in the *red frame* are created by new-coming style transfer; the others are created by existent style transfer

may creates unnatural shapes, such as the created shapes in the first column and last row in Fig. 11a. This is because our method cannot automatically determine the visually reasonable relative size of the style part and content part of novel shapes. Last, to separate styles and contents in the initial set, the input shapes are required to be formed by the proposed styles and contents; otherwise our method may fail.

Future work. To handle complex shapes, it is worth trying to develop a new dense correspondence method. Another interesting direction is how to analyze a set of shapes with global abstract style, such as architecture style, and transfer this type of style to generate richer models. Moreover, we will explore whether it is feasible to analyze the content and style of a set of scenes and create new scenes composed of different styles and contents.

Acknowledgments This work was supported partly by grants from National Natural Science Foundation of China (61003137, 61202185, 61005018, 91120005), Northwestern Polytechnical University Basic Research Fund (310201401JCQ01009, 310201401JCQ01012), the Fundamental Research Funds for the Central Universities, Shaanxi Natural Science Fund (2012JQ8037), and Open Project Program of the State Key Lab of CAD&CG (A1306), Zhejiang University, Program for New Century Excellent Talents in University under grant NCET-10-0079, and Doctoral Fund of Ministry of Education of China under grant 20136102110037.

References

1. Attene, M., Falcidieno, B.: Remesh: An interactive environment to edit and repair triangle meshes. In: Proceeding of Shape Modeling International, pp. 41–46 (2006)
2. Aubry, M., Schlickewei, U., Cremers, D.: The wave kernel signature: a quantum mechanical approach to shape analysis. In: ICCV Workshops, pp. 1626–1633 (2011)
3. Besl, P.J., McKay, N.D.: A method for registration for 3-D shapes. IEEE Trans. Pattern Anal. Mach. Intell. **14**(2), 239–256 (1992)
4. Blanz, V., Vetter, T.: A morphable model for the synthesis of 3D faces. In: Proceedings of SIGGRAPH, pp. 187–194 (1999)
5. Brand, M., Hertzmann, A.: Style machines. In: Proceedings of SIGGRAPH, pp. 183–192 (2000)
6. Bronstein, A.M., Bronstein, M.M., Kimmel, R., Mahmoudi, M., Sapiro, G.: A gromov-hausdorff framework with diffusion geometry for topologically-robust non-rigid shape matching. Int. J. Comput. Vision Mmanuscr. **89**(2–3), 266–286 (2010)
7. Chaudhuri, S., Kalogerakis, E., Guibas, L., Koltun, V.: Probabilistic reasoning for assembly-based 3D modeling. ACM Trans. Graphics **30**(4), 35:1–35:10 (2011)
8. Donoho, D.: De-noising by soft-thresholding. IEEE Trans. Inf. Theory **41**(3), 613–627 (1995)
9. Elgammal, A.M., Lee, C.S.: Separating style and content on a nonlinear manifold. In: Proceedings of IEEE Conference on Computer Vision and Pattern Recognition, pp. 478–485 (2004)
10. Halkidi, M., Batistakis, Y., Vazirgiannis, M.: On clustering validation techniques. J. Intell. Inf. Syst. **17**(2–3), 107–145 (2001)
11. Huang, H., Gong, M., Cohen-Or, D., Ouyang, Y., Tan, F., Zhang, H.: Field-guided registration for feature-conforming shape composition. ACM Trans. Graphics **31**, 171:1–171:11 (2012)
12. Jain, V., Zhang, H.: Robust 3d shape correspondence in the spectral domain. In: Proceedings of Shape Modeling International, pp. 118–129 (2006)

13. Jain, V., Zhang, H.: A spectral approach to shape-based retrieval of articulated 3D models. Comput. Aided Design **39**(5), 398–407 (2007)
14. Kalogerakis, E., Chaudhuri, S., Koller, D., Koltun, V.: A probabilistic model of component-based shape synthesis. ACM Trans. Graphics **31**(4), 55:1–55:11 (2012)
15. Kolmogorov, V., Zabih, R.: What energy functions can be minimized via graph cuts. IEEE Trans. Pattern Anal. Mach. Intell. **26**(2), 65–81 (2004)
16. Kortgen, M., Novotni, M., Klein, R.: 3D shape matching with 3D shape contexts. In: Proceedings of Central European on Computer Graphics (2003)
17. Li, H., Zhang, H., Wang, Y., Cao, J., Shamir, A., Cohen-Or, D.: Curve style analysis in a set of shapes. Comput. Graphics Forum **32**(6), 77–88 (2013)
18. Osada, R., Funkhouser, T., Chazelle, B., Dobkin, D.: Shape distributions. ACM Trans. Graphics **21**(4), 807–832 (2002)
19. Otsu, N.: A threshold selection method from gray-level histograms. IEEE Trans. Syst. Man Cybern. **9**(1), 62–66 (1979)
20. Ovsjanikov, M., Ben-Chen, M., Solomon, J., Butscher, A., Guibas, L.J.: Functional maps: a flexible representation of maps between shapes. ACM Trans. Graphics **31**(4), 30:1–30:11 (2012)
21. Rustamov, R.M., Ovsjanikov, M., Azencot, O., Ben-Chen, M., Chazal, F., Guibas, L.: Map-based exploration of intrinsic shape differences and variability. ACM Trans. Graphics **32**(4), 72:1–72:12 (2013)
22. Shamir, A.: A formulation of boundary mesh segmentation. In: Proceedings of International Symposium on 3D Data Processing, Visualization and Transmission, pp. 82–89 (2004)
23. Shapira, L., Shamir, A., Cohen-Or, D.: Consistent mesh partitioning and skeletonisation using the shape diameter function. Visual Comput. **24**(4), 249–259 (2008)
24. Shilane, P., Funkhouser, T.: Distinctive regions of 3D surfaces. ACM Trans. Graphics **26**(2), 1–15 (2007)
25. Shilane, P., Min, P., Kazhdan, M., Funkhouser, T.: The Princeton shape benchmark. In: Proceedings of Shape Modeling International, pp. 167–178 (2004)
26. Tanenbaum, J., Freeman, W.: Separating style and content with bilinear models. Neural Comput. **12**(6), 1247–1283 (2000)
27. Wang, J.M., Fleet, D.J., Hertzmann, A.: Multifactor gaussian process models for style-content separation. In: Proceedings of International Conference on Machine learning, pp. 975–982 (2007)
28. Xu, K., Li, H., Zhang, H., Cohen-Or, D., Xiong, Y., Cheng, Z.Q.: Style-content separation by anisotropic part scales. ACM Trans. Graph. **29**(6), 184:1–184:10 (2010)
29. Xu, K., Zhang, H., Cohen-Or, D., Chen, B.: Fit and diverse: set evolution for inspiring 3D shape galleries. ACM Trans. Graphics **31**(4), 57:1–57:10 (2012)
30. Zheng, Y., Cohen-Or, D., Mitra, N.J.: Smart variations: functional substructures for part compatibility. Comput. Graphics Forum **32**(2pt2), 195–204 (2013)

Zhizhong Han is a Ph.D. student in the Department of Automation at the NorthWestern Polytechnical University. He received the Bachelor and Master degree majored on Electrical Engineering and Automation. His research interest includes geometric processing, computer vision and machine learning.

Zhenbao Liu received the Ph.D. degree in computer science from the College of Systems and Information Engineering, University of Tsukuba, Japan, in 2009. He is an associate professor at Northwestern Polytechnical University, Xi'an. His research interests include 3D shape analysis, matching, retrieval and segmentation.

Junwei Han currently, is a professor of NorthWestern Polytechnical University. He obtained Ph.D. in April 2003. From 2003 to 2010, He worked as a research staff in Nanyang Technological University, Singapore, The Chinese University of Hong Kong, Dublin City University, Ireland, and University of Dundee, UK, respectively. He was also a visiting researcher in Microsoft Research Asia, China, and University of Surrey, UK. He has published nearly 40 refereed technical papers in international journals and conferences. His publications have received around 250 citations internationally. He is holding 4 patents and serving as a reviewer for many major computer vision journals.

Shuhui Bu received the Ph.D. degree in College of Systems and Information Engineering from University of Tsukuba, Japan in 2009. Currently, he is an associate professor at Northwestern Polytechnical University, China. Prior to joining Northwestern Polytechnical University, he was an assistant professor at Kyoto University, Japan. His research includes 3D shape analysis, image processing, and computer vision.